International Journal of Applied Power Engineering (IJAPE)
Vol.7, No.1, April 2018, pp. 10~17
ISSN: 2252-8792 DOI: 10.11591/ijape.v7.i1.pp10-17

Hybrid System Power Generation 'Wind-photovoltaic' Connected to the Electrical Network 220 kV

Mida Dris[1], Benattous Djilani[2]
[1]Department of Electrical Engineering, University Mohamed Khider, Biskra, Algeria
[2]Department of Electrical Engineering, University EChahid Hamma Lakhdar d'El Oued, Algeria

Article Info

Article history:

Received May 7, 2017
Revised Jan 9, 2018
Accepted Feb 10, 2018

Keyword:

Electrical network 220 kV
Hybrid system
MPPT
Photovoltaic
Renewable energy
Solar
Wind

ABSTRACT

Renewable energy have the potential to generate electricity cleanly without pollution and a lesser dependence of resources for this production of electric power by these systems sources such as solar, wind, hydro, geothermal and biomass instead anti-environmental conventional systems such as gas, coal and oil is a remarkable idea but not frequent in Algeria. Our research focuses on the study of a hybrid energy system (Photovoltaic-Wind), connected to the Electrical Network 220 kV and this by tracking the maximum power point (MPPT) for two energy sources. For this, methods based on optimization algorithms were used side PV array and Wind turbine. With regard to the wind turbine, optimization was based on an analytical approach method. The Matlab/Simulink is used for simulated power output from Hybrid System, power delivered to or from grid and phase voltage of the inverter leg.

Corresponding Author:

Mida Dris,
Department of Electrical Engineering,
University Mohamed Khider, Biskra, Algeria.
Email: midadris@gmail.com, dbenattous@yahoo.fr

1. INTRODUCTION

The literature shows that the cost of renewable energy sources is not necessarily competitive with fossil energy sources, but the need for cleaner energy has generated a proliferation of applications in use renewable energy. They will become, In the future increasingly competitive in terms of technology and production costs and this solution allows the exploitation of local resources for autonomous systems. All renewable energy (solar, hydro wind, biomass) come from the sun [1-4], then transformed by the Earth's environment. Thus, solar and wind energies are more developed and have many advantages. However, we must distinguish several problems depending on the site and renewable energy use. Intermittent availability of such resources leads to the storage problem and correct sizing to reduce the investment cost but also ensure consumer demand. It also raises the problem of coupling between multiple sources to compensate for one another. Our work combines two sources of electrical energy production, namely wind and photovoltaic, which will be connected to the transport network. Boost converter and MPPT method are used to extracted the maximum power from the PV array and the wind turbine [5].

2. PV GENERATION SYSTEM

Photovoltaic cell can be represented by one or two diode connected in parallel with a current source. Figure 1 shows equivalent circuit of PV Array.

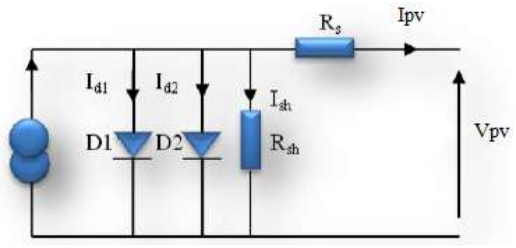

Figure 1. Equivalent circuit of a solar cell

Output current of Photovoltaic panels can be calculated as

$$I_{pv} = I_{ph} - I_{d1} - I_{d2} - I_{sh} \quad (1)$$

The electric current produced by the cell is then given by the following expression:

$$I_{pv} = I_{ph} - I_{s1}\left(\exp\left(\frac{V_{pv} + R_s I_{pv}}{V_t . n_1}\right) - 1\right) - I_{s2}\left(\exp\left(\frac{V_{pv} + R_s I_{pv}}{V_t . n_2}\right) - 1\right) - \left(\frac{V_{pv} + R_s I_{pv}}{R_{sh}}\right) \quad (2)$$

Where:
I_{ph}: Current photonics.
I_{d1}: Current in the diode 1.
I_{d2}: Current in the diode 2.
R_s: Serial Resistance (Ω).
R_{sh}: Shunt Resistance (Ω).

Photonic power is linked to the illumination, temperature and photonic power measured at reference conditions and it is given by:

$$I_{ph} = \frac{G}{G_{ref}}\left(I_{ph(ref)} - \mu_{cc}(T_c - T_{c(ref)})\right) \quad (3)$$

Where:
$I_{ph(ref)}$: Photonic Power on condition of reference [A]
μ_{cc} : : The intensity at temperature sensitivity coefficient [A/K]
G, G_{ref}: :The actual illumination to the reference condition [W/m²]
$T_c, T_{c(ref)}$: Temperature actual cell and the reference condition.

Saturation currents I_{s1} and I_{s2} are given by the following relationships [5]:

$$I_{s1} = C_{s1} . T_c^{\,3} . \exp\left(\frac{-E_{gap} . q}{n_1 . T . k}\right) \quad (4)$$

$$I_{s2} = C_{s2} . T_c^{\,3/2} . \exp\left(\frac{-E_{gap} . q}{n_2 . T . k}\right) \quad (5)$$

Constants C_{s1} and C_{s2} are usually respectively (150-180) $A.K^3$ and (1.3-1.7)x10^{-2} $A.K^{-5/2}$ for a module of 100 cm². A value of the different n of unity duality factor is associated with a predominant recombination mechanism and it depends on the nature and position of the traps levels.
n=1 : The area of space charge is depopulated (ideal case).
1<n< 2 : The trap level is shallow in the area of space charge and n depends on the polarization [6].
n=2 : Recombination centres are distributed evenly in the charging area of space and on a single level in the middle of the band gap.
2<n< 4 : Recombination centres are distributed non-uniformly with a reduced density in the center of the area of space from the surface charge.
E_{gap} : Energy Gap (crystalline silicon=1,12 eV, amorphous silicon=1,7 eV).

2.1. PV MPPT algorithm

As shown in the graph of Figure 2, a perturbation of the power is created and the voltage is incremented or decreased until reaching the maximum point [10-19].

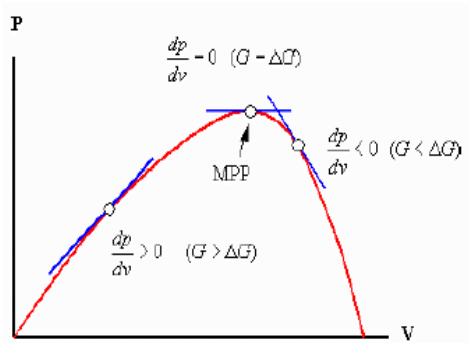

Figure 2. Power versus voltage for perturb and observe algorithm [10]

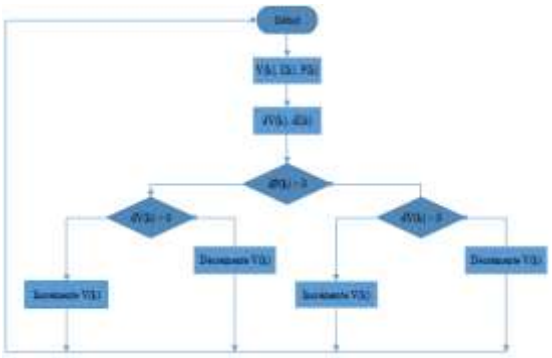

Figure 3. Perturb and observe algorithm

3. WIND SYSTEM

The kinetic energy of the wind collected by the three blades of the wind turbine is converted into mechanical energy through the rotor using a speed multiplier located inside the nacelle finally converted into electricity. The permanent magnet synchronous generator (PMSG) is used to produce this energy because it offers better performance thanks to its higher efficiency because it has no rotor current and can be used without a gearbox, which also implies the Reduction of weight of the nacelle, and reduction of costs. The equivalent circuit of the wind turbine is represented as shown in Figure 4.

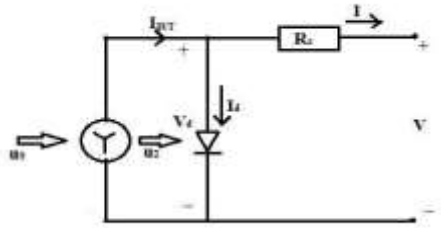

Figure 4. Equivalent circuit of wind turbine

$$P_w = \frac{1}{2}\left[m(\mu_0 - \mu_2)\right] \quad (6)$$

$$P_0 = \frac{1}{2}\left[\rho A \mu_0\right]^3 \quad (7)$$

$$P(t) = \eta_w.\eta_g.0{,}5.\rho\ .C_P.A.V_{r2} \quad (8)$$

Where:

P_w : Output power of turbine
P_0 : Extracted output from wind.
P_{wt} : Generated output power.
η_w. : Efficiency of turbine
η_g. : Efficiency of generator
ρ : Density of air.
C_P : Power co-efficient of wind.
A :Wind turbine swept area.

3.1. Wind MPPT by knowing the characteristic curve $C_P(\lambda)$:

This approach is widely used to avoid the measure of the wind speed to have the expensive anemometers. For low and medium power systems, multi pole permanent magnet synchronous generator are the most recommended, their control is based on the regulation of the excitation of the rotor. The objective of this command is to impose a reference torque so as to enable the wind turbine to rotate at an adjustable speed for low and moderate winds in order to ensure an optimum operating point in terms of extraction. Then to keep this power constant at PN for the strongest winds.

3.2. Indirect control by the steering of the current

One of the main goals of this part of the study is to simplify the structure of the conversion chain of energy dedicated to low wind. This is necessary to reduce the cost without too much diminishing the efficiency of this system. Configurations based on a rectifier bridge with six controlled switches are expensive, include devices of mechanical measures, and require a quite complex control circuit. This controlled rectifier is replaced by a three-phase rectifier diodes. Of the fact, that the diode bridge is an uncontrolled element, the direct autopilot of the generator torque or speed is no longer possible. Another way (indirect) action is therefore necessary. For this, we used a boost converter. The structure seen in this paragraph is given by Figure 5.

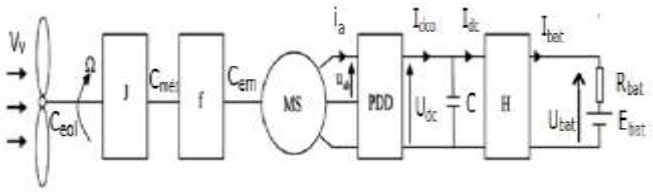

Figure 5. Diagram of a wind turbine conversion chain, with diode rectifier and chopper

$$P_{bat} = U_{bat}.I_{bat} = \eta.C_{eol}.\Omega = \eta.P_{eol} \tag{9}$$

The total yield η is calculated according to the following expression:

$$\eta = \frac{P_{bat}^{\max}}{P_{eol}^{opt}} \tag{10}$$

Where :

$$P_{opt} = \frac{\Omega_{opt}^{3}}{K_{opt}} \tag{11}$$

$$K_{opt} = \frac{2\lambda^3}{\rho A R^3 C_{p\max}} \tag{12}$$

Then we deduce that the maximum power injected into the battery is:

$$P_{bat}^{\max} = \eta \frac{\Omega_{opt}^{3}}{K_{opt}} \tag{13}$$

Thus we can deduce the expression of optimal current in the battery. If we consider that losses are also changing in the cube of the speed, we can define a constant modified K_{opt}:

$$I_{bat}^{opt} = \eta \frac{\Omega_{opt}^{3}}{U_{bat}.K_{opt}} = K'_{opt}.\Omega_{opt}^{3} \tag{14}$$

The search for maximum power device can be built using the measure of the rotation speed of the rotor, such as:

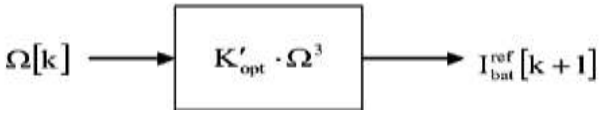

Figure 6. Reference current according to rotation speed

The conversion chain can still be simplified if we consider that the image of the speed of rotation is given by the electromotive forces of the generator. Mechanical speed sensor can be removed and replaced by measuring the continuous U_{dc} bus voltage. This can be likened to the image of the speed of rotation as shown in the equation below.

$$U_{dc}(\Omega) = \frac{3}{\pi}.E_{ab}{}^{\max} = \frac{3\sqrt{6}}{\pi}\psi_{eff}.k.\Omega \tag{15}$$

Then :

$$\Omega = \frac{U_{dc}}{\frac{3\sqrt{6}}{\pi}\psi_{eff}.k} \tag{16}$$

Where
k : : Coefficient of the synchronous generator.

The MPPT control algorithm may result in the following diagram:

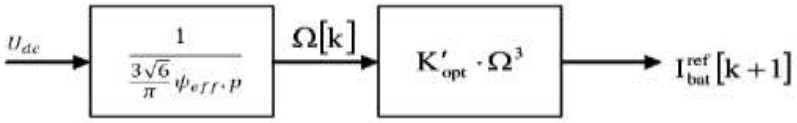

Figure 7. Reference current according to bus voltage

4. DC-DC BOOST CONVERTER

The equivalent dc -dc converter scheme is shown in Figure 8 [10]. When the switch is closed for the duration αT_e, the current in the inductance increases linearly. The voltage at the terminals of K is zero. During the time $t \in [\alpha T_e, T_e]$, the switch opens and the energy stored in the inductance controls the current flow in the free wheel diode D. We have then $V_k = V_o$. By writing that the voltage at the terminals of the inductor is zero, we arrive at:

$$V_o(1-\alpha) = V_i \tag{17}$$

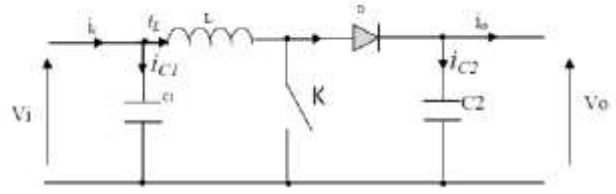

Figure 8. Equivalent circuit of a boost converter

5. HYBRID WIND/PV SYSTEM MODEL

Our hybrid system consists of a wind turbine coupled with a photovoltaic generator connected to the network showing in Figure 9. The AC voltage at the output of the wind turbine is converted into a DC voltage and then coupled with it to the output of the photovoltaic generator. The new DC voltage is converted into an AC voltage by using a three-phase inverter and is connected to the network. The MATLAB-Simulink of hybrid wind/PV system connected with grid is shown in Figure 10.

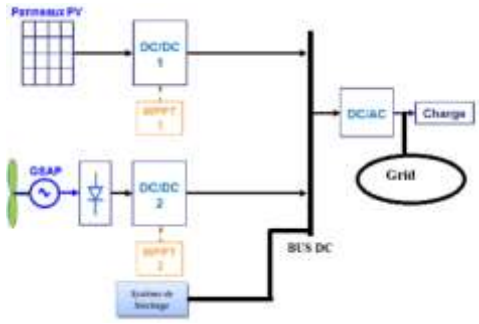

Figure 9. Diagram of proposed system

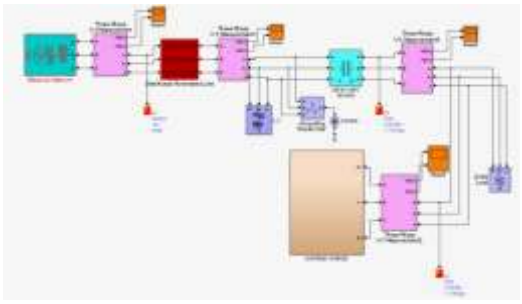

Figure 10. Matlab simulink of hybrid wind/PV system

6. SIMULATION RESULT AND ANALYSIS

After execution of the simulation, Figures below watch the variation of current and voltage in pu of Hybrid Wind/PV system Grid connected. In Figure 12 shows three phase line output voltage and current of hybrid wind/PV system in pu.

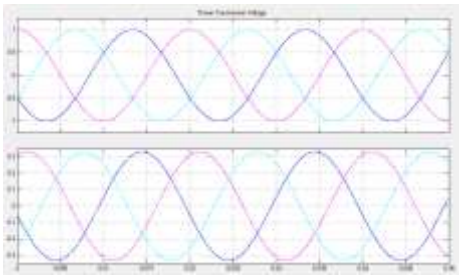

Figure 11. Output current and voltage in pu of hybrid wind/PV system grid connected

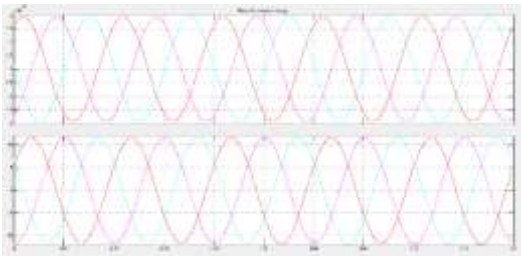

Figure 12. Three phase line output voltage and current of hybrid wind/PV system

Changes in active and reactive powers, the electric torque, the mechanical torque and the wind generation rotation speed are shown respectively in Figures 13 and 14. Figure 15(a) shows the variation of duty cycle and active power generated for the photovoltaic system. In Figure 15(b), it is clear that the DC voltage of the hybrid system output follows a reference voltage (605 V), which shows the electrical stability of the system.

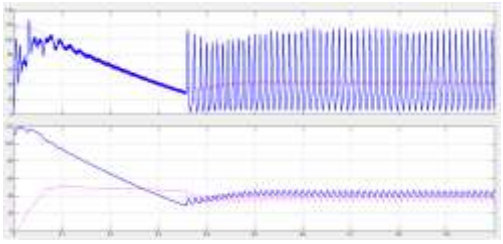

Figure 13. Changes in electric torque, mechanical torque for wind generation

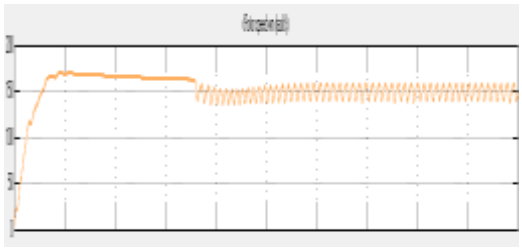

Figure 14. Wind generation rotation speed

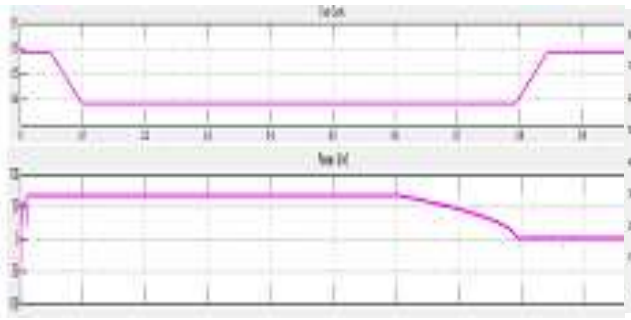

Figure 15(a). Duty cycle and active power generated for the photovoltaic system

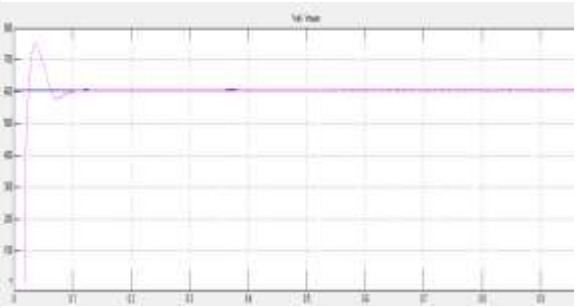

Figure 15(b). Variation in the DC voltage at the output of the hybrid system

7. CONCLUSION

In this work, a brief description of the hybrid systems for the generation of electrical energy is carried out, the main concepts related to the type of architecture of these systems have also been presented. Subsequently, a simulation of a hybrid wind-photovoltaic system was developed, under the Simulink interface of Matlab. The results show that the combination of renewable energy sources in the presence of a storage system with a remarkable advantage in order to reduce the emission of greenhouse gases in addition to the diversity of resources Energy systems, a continuity and availability of power generation is ensured.

We used a DC bus which receives the energy produced by the photovoltaic and wind power sources after convert it at the AC, and then delivered to the consumer or to the network. We also used a load-shedding resistor that allows to dissipate excess energy in the event of a drop in demand and of solid batteries. Several simulation results were presented which illustrated the performance of our installation in the presence of climatic changes and variations in energy consumption.

REFERENCES

[1] C. Darras, "Modélisation de Systèmes Hybrides Photovoltaïque / Hydrogène: Applications site isolé, micro-réseau, et connexion au réseau électrique dans le cadre du projet PEPITE," Thèse de Doctorat, Université de Corse-Pascal Paoli, May 2011.

[2] H. Hassini, "Modelisation, Simulation et Optimisation d'un Systeme Hybride Eolien-Photovoltaique," Memoire de Magister, Université Abou-Bakr Belkaid de Tlemcen,2010.

[3] M. Muralikrishnan and V. Lakshminarayana, "Hybrid (Solar and Wind) Energy System for Rural Electrification," *ARPN Journal of Engineering and Applied Sciences*, vol. 3, no. 5, pp 50-58, October 2008.

[4] Mida Dris, Ben Attous Djilani, "Comparative Study Of Algorithms (MPPT) Applied To Photovoltaic Systems" *International Journal of Renewable Energy Research*, vol. 3, no. 4, pp. 872-879, 2013.

[5] Grégoire Léna (IED), "Mini-réseaux hybrides PV-diesel pour l'électrification rurale," rapport AEI-PVPS T9-13:2013 CLUB-ER, no, pp12-13, Juillet 2013.

[6] Majid Jamil, Ravi Gupta, "A review of power converter topology used with PMSG based wind power generation," IEEE, 2012

[7] Swapneel kaurav, Prof.P.Yadav," Hybrid Power System Using Wind Energy and Solar Energy", *International Journal of Innovative Research in Science, Engineering and Technology*, vol. 5, no. 1, Januray 2016.

[8] H. H. El-Tamaly and A. A. Elbaset Mohammed, "Modeling and simulation of Photovoltaic/Wind Hybrid Electric Power System Interconnected with electrical utility," *2008 12th International Middle-East Power System Conference*, Aswan, 2008, pp. 645-649.

[9] E. I. Ortiz-Rivera, "Maximum power point tracking using the optimal duty ratio for DC-DC converters and load matching in photovoltaic applications," *2008 Twenty-Third Annual IEEE Applied Power Electronics Conference and Exposition*, Austin, TX, 2008, pp. 987-991.

[10] A.Hina Fathima et al, "Optimization in micro grids with hybrid energy systems ». School of Electrical Engineering," VIT University, Vellore, India, 2015.

[11] M. Jamil, R. Gupta and M. Singh, "A review of power converter topology used with PMSG based wind power generation," *2012 IEEE Fifth Power India Conference*, Murthal, 2012, pp. 1-6.

[12] M. Gengaraj, J. Jasper Gnanachandran, "Modeling of a standalone photovoltaic system with charge controller for battery energy storage system," *International Journal of Electrical Engineering* , vol. 6, no. 3, pp. 259-268, 2013.

[13] J. Kasera, A. Chaplot and J. K. Maherchandani, "Modeling and simulation of wind-PV hybrid power system using Matlab/Simulink," *2012 IEEE Students' Conference on Electrical, Electronics and Computer Science*, Bhopal, 2012, pp. 1-4.

[14] S. Meenakshi, K. Rajambal, S. Elangovan, "Intelligent controller for stand – alone hybrid generation system," IEEE May.2006.

[15] S. Meenakshi, K. Rajambal, C. Chellamuthu and S. Elangovan, "Intelligent controller for a stand-alone hybrid generation system," *2006 IEEE Power India Conference*, New Delhi, 2006, pp. 8 pp.-.

[16] Christian Kanchev, "Gestion des flux énergétiques dans un système hybride de sources d'énergie renouvelable : Optimisation de la planification opérationnelle et ajustement d'un micro réseau électrique urbain", doctorat délivré simultanément par l'école centrale de Lille et l'université technique de Sofia le 24 janvier 2014.

[17] Mimi Belatel et Abdelghani Ouazeta, " Study of The Different Stages of A Hybrid System (Photovoltaic Wind Fuel Cell) in French*: Etude des différents étages d'un système hybride (photovoltaïque – éolien – pile à combustible)*," *Communication Science & technologie*, vol. 14, pp. 1-11, January 2014.

[18] A. Tani, M. B. Camara and B. Dakyo, "Energy Management in the Decentralized Generation Systems Based on Renewable Energy—Ultracapacitors and Battery to Compensate the Wind/Load Power Fluctuations," in *IEEE Transactions on Industry Applications*, vol. 51, no. 2, pp. 1817-1827, March-April 2015.

[19] Aditi; Dr. A. K. Pandey, "Performance Analysis of grid connected PV Wind Hybrid Power System,", *International Journal of Applied Engineering*,vol. 11, no. 1, pp. 706-712, 2016.